

Application of Self-Organizing Maps for clustering DJIA and NASDAQ100 portfolios

A.A.Zherebtsov*, Yu.A.Kuperin#

* Division of Computational Physics, Department of Physics,
St.Petersburg State University, St.Petersburg 198904, Russia
e-mail: jerebtsov@AZ9629.spb.edu

#Laboratory of Complex Systems Theory, Institute of Physics,
St.Petersburg State University, St.Petersburg 198904, Russia
e-mail: kuperin@JK1454.spb.edu

Abstract

In this paper we apply the Self -Organized Map (SOM) method for clustering the DJIA and NASDAQ100 portfolios for determination of non-linear correlations between stocks. We represent the application of this method as alternative to ultrametric spaces method. We have found , that SOM method is more relevant and perspective for clustering ill-structured large databases and, in particular, NASDAQ100, where nonlinear processing of the large data samples is required.

1 Introduction

Usually the process of data analysis or extraction of knowledge from the data consists of a number of iterative steps, since the formulation of the purposes depends in some respects on the obtained results. It can include a loop of a feedback that means reformulation the purposes on the basis of the received information. Depending on the purposes and complexity of the data it is possible to use any type of well-known algorithms based on recognition of images, machine training or the multivariate statistical analysis. The key point here is the detection of originally unknown structures or patterns in the analyzed data.

The most popular and simple approach to generalization of data sets is statistical tables. Elementary of them allows to obtain the statistics of the data. It could be, for example, the minimum and maximum values in a data set, a median, the first and the third quartile etc. It works well for linear data sets of small dimension. However it remains the rather important combined practical problem of generalization and visualization of the multidimensional data sets.

The Self-Organizing Map represents the result of a vector quantization algorithm that places a number of reference or codebook vectors into a high-dimensional input data space to approximate to its data sets in an order fashion (Kohonen, 1982,1990,1995, Kohonen, Oja, et al, 1996). When local-order relations are defined between the reference vectors, the relative values of the latter are made to depend on each other as if their neighboring values would lie along an "elastic surface". By means of the self-organizing algorithm, this "surface" becomes defined as a kind of nonlinear regression of the reference vectors through the data points. A mapping from a high-dimensional data space into a two-dimensional lattice of points is thereby also defined. Such a mapping can effectively be used to visualize metric ordering relations of input samples. The self-organized map algorithm has been used for a wide variety of applications, mostly for engineering problems but also for data analysis (Back, et al (1996), Demartines (1994), Carlson

(1991), Cheng, et al (1994), Garavaglia (1993), Martín-del-Brío, Serrano-Cinca (1993), Marttinen (1993), Serrano-Cinca (1996), Ultsch (1993), Ultsch, et al (1990), Varfis, et al (1992), Zhang, Li, (1993), Deboeck, Kohonen (1998)).

In Mantegna, Stanley (2001) the method of ultrametric spaces was used for clustering of DJIA and NASDAQ500 portfolios. In the present paper we apply both the ultrametric spaces approach and SOM algorithms for clustering the DJIA and NASDAQ100. We compare these approaches and show, that in contrast to the ultrametric spaces method the SOM algorithms are more perspective for clustering NASDAQ100 where processing of the large data samples is required. It is due to the linear character of methods of hierarchical trees and intrinsically nonlinear processing of information by any neural network and by SOM, in particularly. Finally SOM can learn from the data, i.e. it is adaptive algorithm for data clustering or quantization whereas the ultrametric spaces method is not.

The paper is organized as follows. In Sections II and III, we review the basics principles of SOM and ultrametric spaces methods accordingly. In Section IV, we present the study of the DJIA index using ultrametric spaces method. In Section V, clusterization of DJIA by SOM method is represented. Sections VI and VII, presents clusterization of NASDAQ100 by ultrametric spaces and SOM methods accordingly. In Section VIII some conclusions are given.

2 The principle of SOM

SOM is a kind of neural network learning without a supervisor (Kohonen, 1982,1990,1995, Kohonen, Oja, et al, 1996). Adapting to the training set SOM forms its outputs by itself. The basic SOM consists of M neurons located on a regular low-dimensional lattice, usually 1- or 2-dimensional. Higher dimensional lattices are possible, but they are not generally used since their visualization is problematic. The lattice is usually either hexagonal or rectangular.

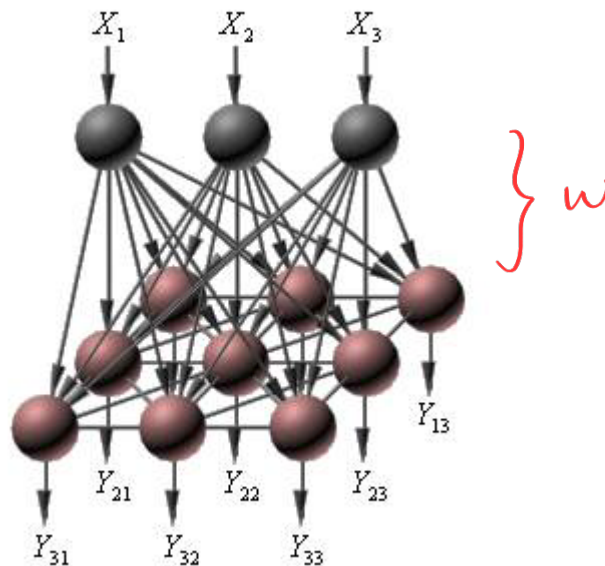


Figure 1.

The schematic architecture of Self-Organized Map.

Gray balls form the input layer, and brown ones form the output layer. Arrows connecting input and output layers are connections with its own weights.

(After Shumsky et al (1998)).

It is well-known (Kohonen (1995)) that SOM performs two types of data compression:

- reduction of data dimension with minimum lost of information. (This neural networks can single out sets of independent characteristics);
- reduction of data variety due to terminal composition prototypes separation. (Clustering and quantization of data sets);

The basic SOM algorithm is iterative. Each neuron i has a d -dimensional prototype vector $\mathbf{w}_i = [w_{i1}, \dots, w_{id}]$ or weight of i -th neuron. At each training step, a sample data vector \mathbf{x} is randomly chosen from the training set. Distances between \mathbf{x} and all the prototype vectors are computed. The best-matching unit (BMU) or the winner unit, denoted here by \mathbf{x}_{i^*} is the map unit with prototype closest to \mathbf{x} (Kaski (1997)):

$$|\mathbf{w}_{i^*} - \mathbf{x}| \leq |\mathbf{w}_i - \mathbf{x}|, \forall i \neq i^*.$$

Next, the prototype vectors are updated. The BMU and its topological neighbors are moved closer to the input vector in the input space by the rule $\Delta \mathbf{w}_{i^*}^r = \eta(\mathbf{x}^r - \mathbf{w}_{i^*})$, where. η is learning rate and $\Delta \mathbf{w}_{i^*}^r$ is modification of i -th neuron weight.

Finally, the update rule for the all vectors of unit i is:

$$\Delta \mathbf{w}_i^r = \eta \Lambda(|\mathbf{i} - \mathbf{i}^*|) (\mathbf{x}^r - \mathbf{w}_i),$$

where $\Lambda(|\mathbf{i} - \mathbf{i}^*|)$ is a neighborhood kernel centered on a winner unit. The kernel can be for example Gaussian: $\Lambda(a) = \exp(-a^2/\sigma^2)$, where σ is neighborhood radius. Both learning rate η and neighborhood radius σ decrease monotonically in time. During training, the SOM behaves like a flexible net that folds into the "cloud" formed by the training data (Fig. 2). Because of the neighborhood relations, neighboring prototypes are pulled to the same direction, and thus prototype vectors of neighboring units resemble each other. Amount of neurons in output layer defines maximum difference of model vectors. Then trained SOM can classify its inputs: BMU define class of input vectors.

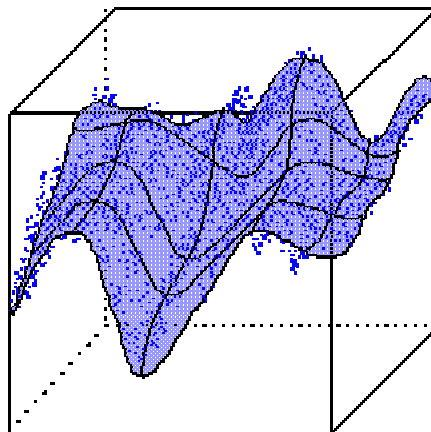


Figure 2.

2-dimensional map of 3-dimensional data set.
(After Shumsky et al (1998)).

The SOM forms a low-dimensional map of training set. The ordered SOM lattice can be used as a convenient visualization platform for showing different features of the SOM (and thus of the data). The goal of visualization is to present large amount of detailed information in order to give a qualitative idea of the properties of the data. Typically the number of properties that need to be visualized is much higher than the number of usable visual

dimensions. It is simply impossible to show them all in a single figure. Every vector from many-dimensional input space have it is own coordinate on the lattice. The closer coordinates of two vectors on the map are, the closer these vectors are in the input space. But the opposite statement is not correct (Fig. 3). Representation reducing dimension and retaining nearness attitude does not exist in general case.

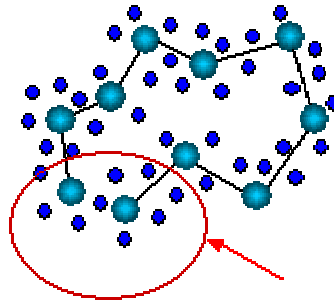


Figure 3.

Close vectors from the input space are reflected on the opposite sides of the map.
(After Shumsky et al (1998)).

It is convenient to visualize SOM like topographic map. Each characteristic of the input data causes its own coloration on the map (Fig. 4) (Kohonen, Oja et al (1996)).

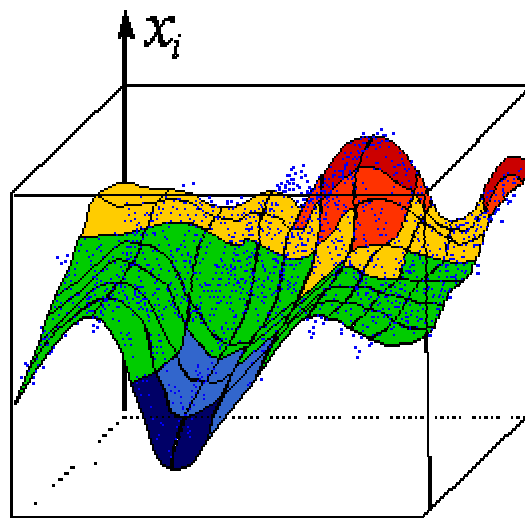


Figure 4.

Coloring of the topographic map induced by i-th component of input data.
(After Shumsky et al (1998)).

3 Ultrametric spaces

In financial markets, huge number of stocks is traded simultaneously. One way to detect similarities and differences in the synchronous time evolution of a pair of stocks is to study the correlation coefficient ρ_{ij} between the daily logarithmic changes in price of two stocks i and j (Mantegna, Stanley (2001)).

Let us define logarithmic return for stock i

$$S_i(t) = \ln Y_i(t) - \ln Y_i(t-1), \quad (1)$$

where $Y_i(t)$ is a daily closure price of stock i at time t ($0 \leq t \leq n$). Correlation coefficient ρ_{ij} between the daily logarithmic changes in price of two stocks i and j is given by:

$$\rho_{ij} = \frac{\langle S_i S_j \rangle - \langle S_i \rangle \langle S_j \rangle}{\sqrt{\langle S_i^2 - \langle S_i \rangle^2 \rangle \langle S_j^2 - \langle S_j \rangle^2 \rangle}} \quad (2)$$

The angular brackets indicate a time average over all the trading days within the investigated time period.

Let

$$\hat{S}_i = \frac{S_i - \langle S_i \rangle}{\sqrt{\langle S_i^2 \rangle - \langle S_i \rangle^2}} \quad (3)$$

Then we can consider $\hat{S}_i(t)$ ($1 \leq t \leq n$) as the vectors $\vec{\hat{S}}_i$ in n -dimensional space (Rammal et al (1986)).

One can set the distance in this space by several well-known ways:

- Euclidean distance: $d_{ij} = \|\vec{\hat{S}}_i - \vec{\hat{S}}_j\| = \sqrt{\sum_{k=1}^n (\hat{S}_{ik} - \hat{S}_{jk})^2}$;
- squared Euclidean distance: $d_{ij} = \|\vec{\hat{S}}_i - \vec{\hat{S}}_j\|^2 = \sum_{k=1}^n (\hat{S}_{ik} - \hat{S}_{jk})^2$;
- City-block (Manhattan) distance: $d_{ij} = \sum_{k=1}^n |\hat{S}_{ik} - \hat{S}_{jk}|$;
- Chebyshev distance: $d_{ij} = \max_k |\hat{S}_{ik} - \hat{S}_{jk}|$;
- Power distance: $d_{ij} = \left(\sum_{k=1}^n |\hat{S}_{ik} - \hat{S}_{jk}|^p \right)^{1/p}$, where r and p are free parameters;
- Pearson distance: $d_{ij} = 1 - \rho_{ij}$, here ρ_{ij} is defined by equation (2).

All distances written above should satisfy the standard properties:

1. $d_{ij} > 0$; $d_{ij} = 0$, если $i = j$;
2. $d_{ij} = d_{ji}$, $\forall i, j$;
3. $d_{ij} \leq d_{ik} + d_{kj}$, $\forall i, j, k$;

An ultrametric space is a space endowed by so-called ultrametric distance. An ultrametric distance \hat{d}_{ij} must satisfy the first two properties of a metric distance, while the usual triangular inequality is replaced by a stronger inequality, called an ultrametric inequality,

$$\hat{d}_{ij} \leq \max_k \{ \hat{d}_{ik}, \hat{d}_{kj} \}.$$

Benzécri (1984) rigorously studied the general connection between indexed hierarchies and ultrametrics. Provided that a metric distance between n objects exists, several ultrametric spaces can be obtained by performing any given partition of n objects. By means of ultrametric spaces one can obtain hierarchical trees.

However, once several objects have been linked together in some clusters, we should determine the distances between those new clusters. In other words, we should determine the rules of amalgamation (linkage rules). Some of these rules are adduced below.

- **Single linkage (nearest neighbor)**
In this method the distance between two clusters is determined by the distance of the two closest objects (nearest neighbors) in the different clusters. This rule will, in a sense, string objects together to form clusters, and the resulting clusters tend to represent long "chains."
- **Complete linkage (furthest neighbor)**
In this method, the distances between clusters are determined by the greatest distance between any two objects in the different clusters (i.e., by the "furthest neighbors"). This method usually performs quite well in cases when the objects actually form naturally distinct "clumps." If the clusters tend to be somehow elongated or of a "chain" type nature, then this method is inappropriate.
- **Unweighted pair-group average**
In this method, the distance between two clusters is calculated as the average distance between all pairs of objects in the two different clusters. This method is also very efficient when the objects form natural distinct "clumps," however, it performs equally well with elongated, "chain" type clusters.
- **Weighted pair-group average**
This method is identical to the unweighted pair-group average method, except that in the computations, the size of the respective clusters (i.e., the number of objects contained in them) is used as a weight. Thus, this method (rather than the previous method) should be used when the cluster sizes are suspected to be greatly uneven.
- **Unweighted pair-group centroid**
The centroid of a cluster is the average point in the multidimensional space defined by the dimensions. In a sense, it is the center of gravity for the respective cluster. In this method, the distance between two clusters is determined as the difference between centroids.
- **Weighted pair-group centroid (median)**
This method is identical to the previous one, except that weighting is introduced into the computations to take into consideration differences in cluster sizes (i.e., the number of objects contained in them). Thus, when there are (or one suspects there to be) considerable differences in cluster sizes, this method is preferable to the previous one.
- **Ward's method**
This method is distinct from all other methods because it uses an analysis of variance approach to evaluate the distances between clusters. In short, this method attempts to minimize the Sum of Squares (SS) of any two (hypothetical) clusters that can be formed at each step. Refer to Ward (1963) for details concerning this method. In general, this method is regarded as very efficient, however, it tends to create clusters of small size.

Ultrametric spaces provide a natural way to describe hierarchically structured complex systems, since the concept of ultrametricity is directly connected to the concept of hierarchy (Rammal et al (1986)).

Hierarchical trees associated with the single linkage between clusters can be obtained as follows. Let the distance matrix be given by table 1.

Table. 1. Distance matrix

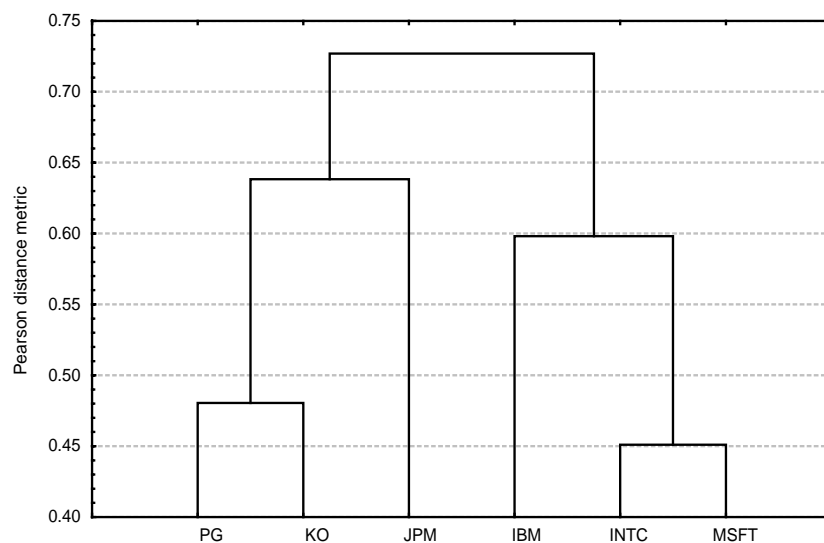
	PG	IBM	MSFT	INTC	KO	JPM
PG	0	1.15	1.18	1.15	0.47	0.64
IBM		0	0.60	0.64	1.26	1.16
MSFT			0	0.45	1.27	1.11
INTC				0	1.26	0.74
KO					0	0.94
JPM						0

To obtain hierarchical tree we find the pair of stocks separated by the smallest distance: INTC and MSFT ($d=0.45$). Then find the pair of stocks with the next-smallest distance: PG and KO ($d=0.47$). Thus we have two separated clusters (KO-PG and INTC-MSFT). If we continue, we find MSFT and IBM ($d=0.60$). At this point our clusters are follows KO-PG and INTC-MSFT-IBM. The next pairs of closest stocks are JPM-PG and INTC-IBM ($d=0.64$). So the two clusters are INTC-MSFT-IBM and JPM-KO-PG. The smallest distance connecting the two clusters is observed for JPM-INTC ($d=0.74$). Table 2 gives matrix of the ultrametric distances.

Table. 2. Matrix of the ultrametric distances

	PG	IBM	MSFT	INTC	KO	JPM
PG	0	0.74	0.74	0.74	0.47	0.64
IBM		0	0.60	0.60	0.74	0.74
MSFT			0	0.45	0.74	0.74
INTC				0	0.74	0.74
KO					0	0.64
JPM						0

In Fig 5 we show the hierarchical tree obtained by the ultrametric method described above (see, also (Mantegna, Stanley (2001))).

Figure 5.
Hierarchical tree.

However this method have some demerits. This caused by variety of distances and distance rules that affect on cluster structure of the hierarchical tree.

4 Study of Dow-Jones Industrial Average Index by ultrametric method

In this section we investigate DJIA by ultrametric method. We obtain cluster structure of this index by building appropriate hierarchical trees.

Let us first normalize $S_i(t)$ given by equation (2) on the interval $[0,1]$ by nonlinear transformation $\tilde{S}_i = f(\frac{S_i - \bar{S}_i}{\sigma_i})$. Here $f(a) = \frac{1}{1 + e^{-a}}$ is the activation function, $\bar{S}_i = \frac{1}{P} \sum_{j=1}^P S_i^j$ is an average of distribution and $\sigma_i = \frac{1}{P-1} \sum_{j=1}^P (S_i^j - \bar{S}_i)^2$ is a root-mean-square deviation (volatility) of the i-th stock.

In this study we use hourly data for DJIA. For the set of 30 stocks of the DJIA (table 3¹), there are $(30 \times 29) / 2 = 435$ different ρ_{ij} . All ρ_{ij} are calculated for each studied time period. In Table 4 maximal and minimal values of ρ_{ij} are summarized. Maximal value $\rho_{ij}=0,61$ from *10-Jan-94 to 27-Oct-97* corresponds to the companies JP Morgan Chase and American Express (Fig. 6). Maximal value $\rho_{ij}=0,72$ from *10-Nov-1997 to 27-Aug-2001* corresponds to the companies JP Morgan Chase and Citigroup (Fig.7). All this companies are engaged in financial services.

Table 3. The set of 30 stocks of the DJIA30.

Ticker	Company	Industry sector
AA	Alcoa inc.	Metallurgy
AXP	American Express	Providing financial service
BA	Boeing	The aerospace industry
C	Citigroup	Providing financial service
CAT	Caterpillar	Mechanical engineering
DD	DuPont	Manufacture of hi-tech materials
DIS	Walt Disney	Showbiz industry
EK	Eastman Kodak	Imaging products and services
GE	General Electric	The electrotechnical company
GM	General Motors	Mechanical engineering
HD	Home Depot	Home improvement retailer
HON	Honeywell International	The aerospace industry
HWP	Hewlett-Packard	Computer technique industry
IBM	International Bus. Machine	Computer technique industry
INTC	Intel	Computer technique industry
IP	International Paper	Paper and packaging company
JNJ	Johnson & Johnson	Cosmetic industry
JPM	JP Morgan Chase	Providing financial service
KO	Coca Cola inc.	Foodstuff industry
MCD	McDonalds Corp.	Foodstuff industry
MMM	Minnesota Mining	Abrasives manufacturing
MO	Philip Morris	Tobacco industry
MRK	Merck & CO	Pharmaceutical products industry
MSFT	Microsoft	Software development
PG	Procter & Gamble	Cosmetic industry
SBC	SBC Communications	Providing of communication
T	AT&T	Providing of communication
UTX	United Technology	The aerospace industry
WMT	Wal-Mart Stores	Operation of mass merchandising stores
XOM	Exxon Mobil	Mining and sale of coal, copper and other minerals

¹ finance.yahoo.com.

Table 4. The observed minimum and maximum values of correlation coefficient ρ_{ij} for 30 stocks of DJIA.

Time period	Min ρ_{ij}	Max ρ_{ij}
from 10-Jan-94 to 27-Oct-97	-0,04	0,61
from 10-Nov-97 to 27-Aug-01	-0,06	0,72

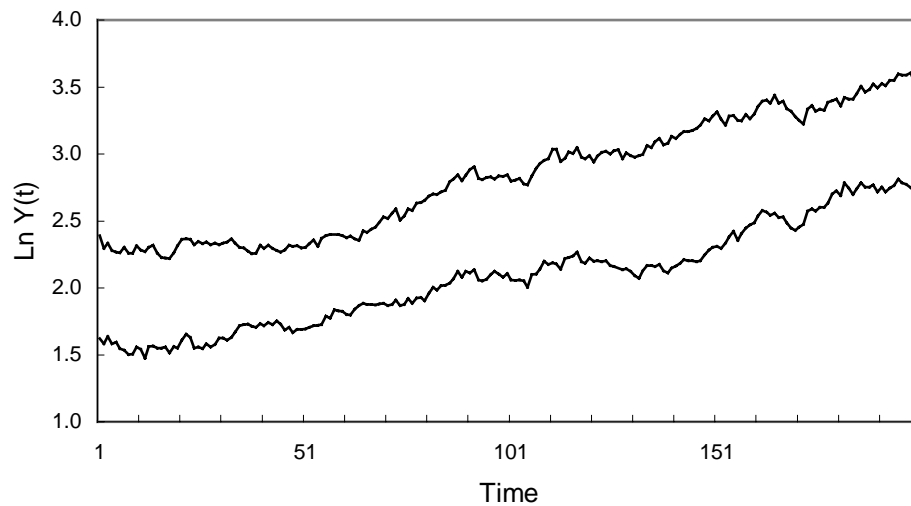


Figure 6.

Time evolution of $\ln Y(t)$ for JP Morgan Chase (top curve) and American Express (bottom curve) from 10-Jan-1994 to 27-Oct-1997.

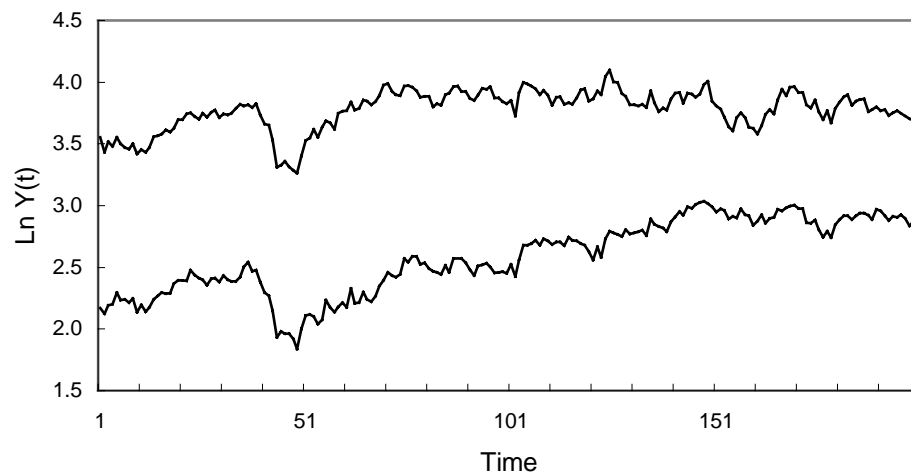


Figure 7.

Time evolution of $\ln Y(t)$ for JP Morgan Chase (top curve) and Citigroup (bottom curve) from 10-Nov-1997 to 27-Aug-2001.

In Figures 8 and 9 hierarchical trees for 30 stocks which composed DJIA from 10-Jan-94 to 27-Oct-97 and from 10-Nov-97 to 27-Aug-01 respectively are represented. Hierarchical trees were constructed on the basis of Pearson distance metric and unweighted pair-group average linkage.

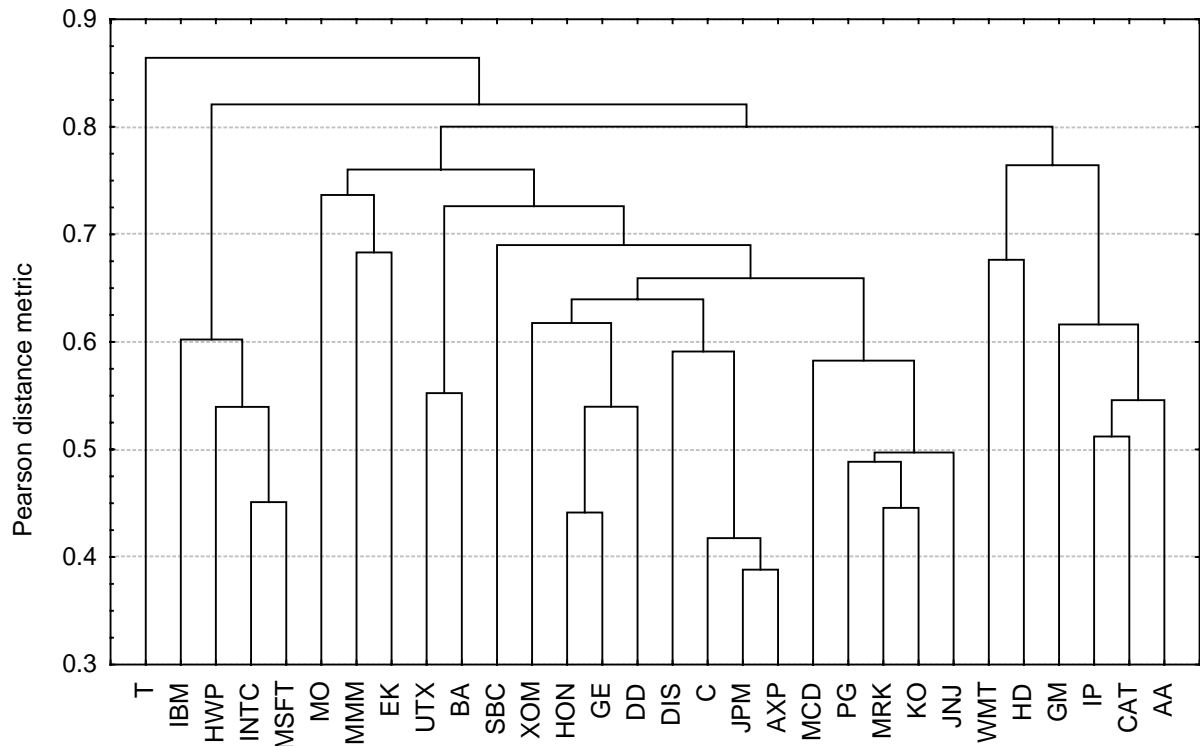


Figure 8.
Hierarchical tree for 30 stocks used to compute the DJIA
 from 10-Jan-1994 to 27-Oct-1997

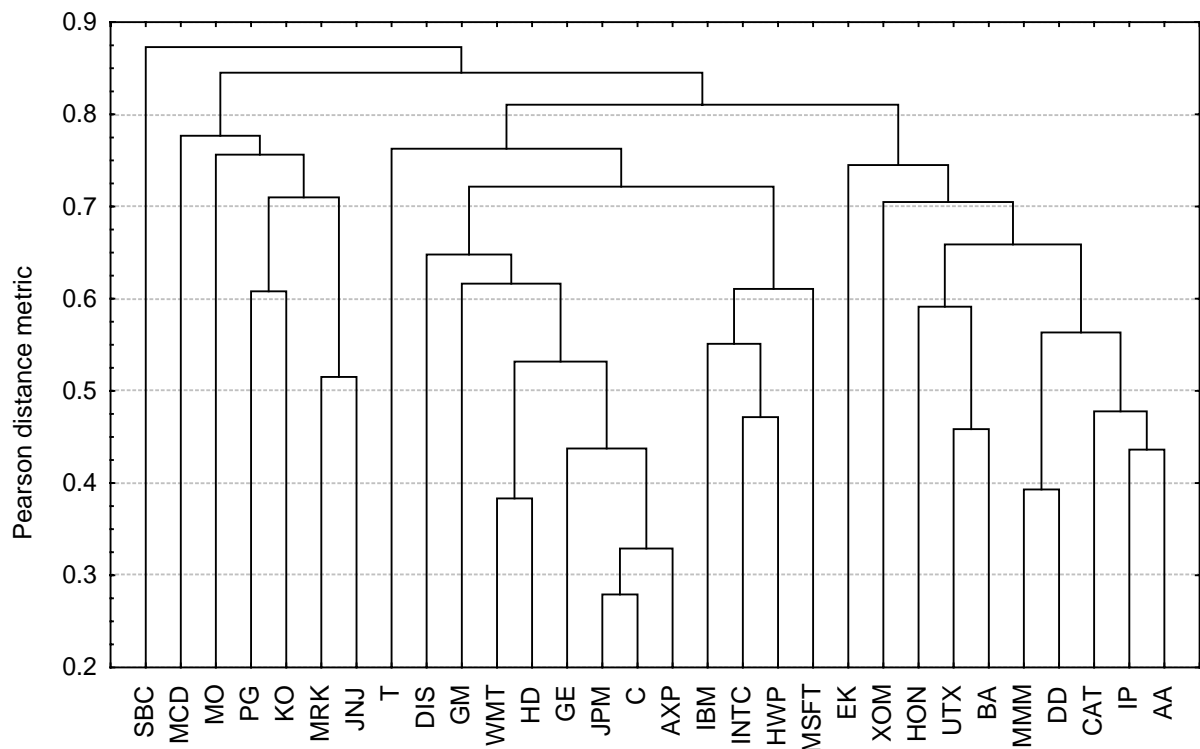


Figure 9.
 Hierarchical tree for 30 stocks used to compute the DJIA
 from 10-Nov-1997 to 27-Aug-2001

Figures 8 and 9 represent cluster structure of the DJIA for each investigated period. As can be seen, financial companies AXP, C and JPM belong to the most correlated cluster. Although

telecommunication companies T (Fig. 8.) and SBC (Fig. 9.) are weakly correlated with other companies.

5 Application of SOM method for clustering DJIA

In the present section we apply Self-Organized Maps method for clustering DJIA and we compare results of this method with results obtained by ultrametric method.

Construction of the SOM consists of two stages:

- 1) choice of parameters of training;
- 2) direct training of SOM.

Process of training includes rough tuning and exact fine-tuning. At a stage of rough tuning rough clusterization of the training set occurs. For this stage large correction of weights of the output layer is occurring. But at the stage of exact turning value of the correction considerably decreases. Experimentally we found that it is desirable, that the number of epochs for rough tuning was in 100 times more then neurons in a map.

The radius of training at the beginning of training should be commensurable with the size of a map, and at the end of training - small enough. Learning rate changes depending on the sizes of a map and the number of epochs. Learning rate can vary by the following rules:

- linear;
- inversely to the number of examples.

We used the second rule because it gives the smoothest change of the weights of neurons.

Initialization of weights of vectors of the SOM can be made by:

- random values;
- examples from the training set.

In the present study we used random values of initialization. Table 5 summaries the parameters of training of the SOM for DJIA.

Table 5. Parameters of training the SOM for DJIA from *10-Jan-94 to 27-Oct-97* and from *10-Nov-97 to 27-Aug-01*.

The size of a map	40x40 neurons
The form of cells	Hexagons
Number of epoch at the rough tuning	100000
Number of epoch at the exact tuning	100000
Learning rate at the rough tuning	0.2
Learning rate at the exact tuning	0.05
Initial radius of training	20
Final radius of training	1
Updating of the learning rate	Inversely proportional
Initial weights initialization	Random values
Time of training	3 hours and 15 minutes

Figures 10 and 11 show the learning error in log-linear coordinates. Namely, the logarithm of an average error of training (average distance between all weight factors of neurons in the SOM and actual values of training samples) versus the number of epochs is shown.

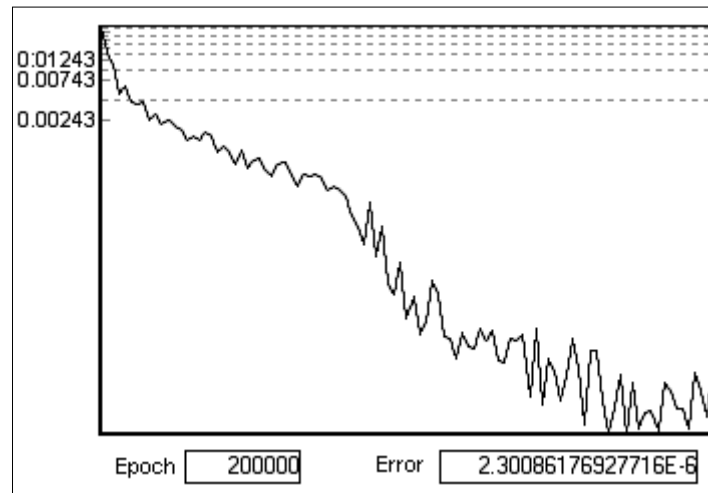


Figure 10.
Learning error for the SOM of DJIA
from 10-Jan-94 to 27-Oct-97.

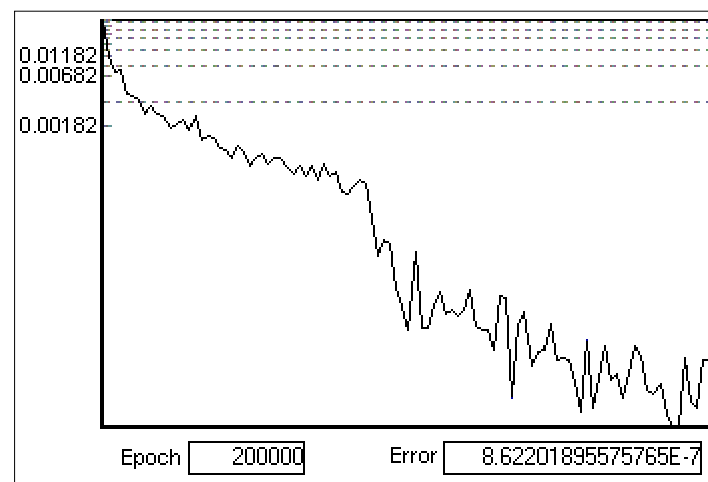


Figure 11.
Learning error for the SOM of DJIA
from 10-Nov-97 to 27-Aug-01.

The U-matrix holds all distances between neighboring map units (Kaski (1997), Graepel et al (1998)). Dark blue color of a map unit means, that the average distance from this unit to its nearest neighbors is not enough. The darkest blue cells correspond to the neural-winners. Red color of a map unit means that the average distance from these cells to their nearest neighbors is large. Cluster is the group of vectors, distances between which inside this group is less, than distances to the next groups. The large difference between color of two clusters means, that these clusters are far apart. Figures 12 and 13 represent the U-matrix, cluster structure of SOM, and the error of clusterization for the both investigated periods. The Figure appropriate to the error of quantization of SOM, shows a distinction between modeling vectors of weights of neural-winners and actual input vectors. Red value of the map unit means, that the vector of weights of this unit is far from a real entrance vector.

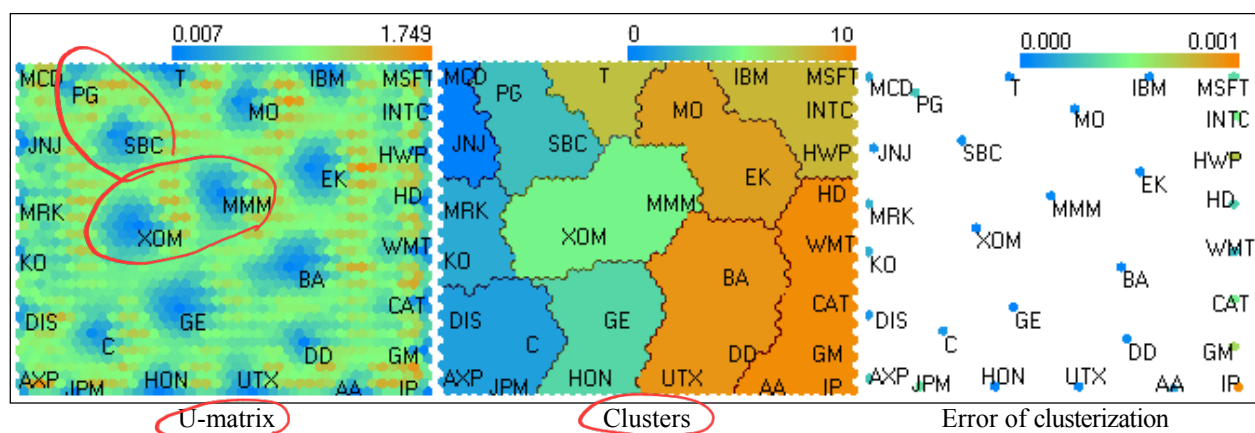


Figure 12.

Self-organized map of DJIA index
from 10-Jan-94 to 27-Oct-97.

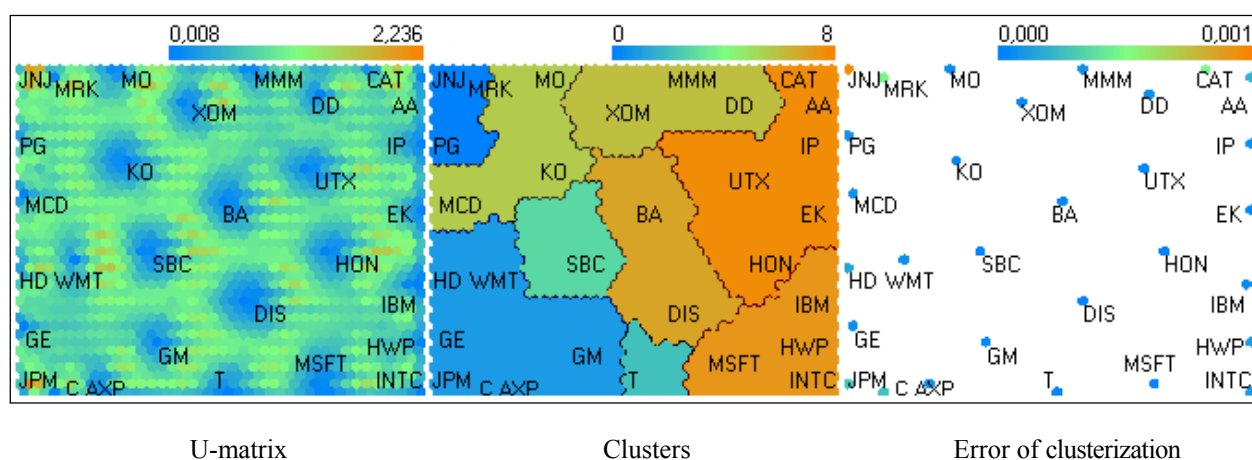


Figure 13.

Self-organized map of DJIA index
from 10-Nov-97 to 27-Aug-01.

The SOM divide all space of the companies on clusters, and everyone cluster includes the companies with high coefficient of correlation. Tables 6 – 8 summarize the correlation matrices for stocks, which are included into one cluster for the period from 10-Jan-94 to 27-Oct-97. Appropriate clusters can be seen also in Figure 8.

Table 6. Correlation matrix for stocks which have got into one cluster from 10-Jan-94 to 27-Oct-97

	AA	CAT	GM	HD	IP	WMT
AA	1	0,48	0,36	0,23	0,43	0,19
CAT		1	0,45	0,38	0,49	0,24
GM			1	0,26	0,34	0,23
HD				1	0,21	0,32
IP					1	0,14
WMT						1

Table 7. Correlation matrix for stocks which have got into one cluster from *10-Jan-94 to 27-Oct-97*

	MSFT	HWP	IBM	INTC
MSFT	1	0,40	0,40	0,55
HWP		1	0,41	0,52
IBM			1	0,38
INTC				1

Table 8. Correlation matrix for stocks which have got into one cluster from *10-Jan-94 to 27-Oct-97*

	AXP	C	DIS	JPM
AXP	1	0,57	0,40	0,61
C		1	0,46	0,60
DIS			1	0,37
JPM				1

In Tables 9 - 11 correlation matrices for groups of stocks, which have fallen into three different clusters for the period from *10-Nov-97 to 27-Aug-01* are given.

Table 9. Correlation matrix for stocks which have fallen into one cluster for the period from *10-Nov-97 to 27-Aug-01*

	AA	CAT	EK	HON	IP	UTX
AA	1,	0,51	0,25	0,24	0,56	0,33
CAT		1	0,34	0,33	0,54	0,44
EK			1	0,31	0,31	0,30
HON				1	0,41	0,47
IP					1	0,36
UTX						1

Note, that shown in Figure 9 cluster BA-MMM-DD-AA-CAT-EK-HON-IP-UTX contains stocks from Table 9 and also stocks BA, MMM and DD from the nearest cluster of SOM.

Table 10. Correlation matrix for stocks which have fallen into one cluster from *10-Nov-97 to 27-Aug-01*.

	MSFT	HWP	IBM	INTC
MSFT	1	0,38	0,31	0,48
HWP		1	0,46	0,53
IBM			1	0,44
INTC				1

Table 11. Correlation matrix for stocks which have fallen into one cluster from *10-Nov-97 to 27-Aug-01*.

	AXP	C	GE	GM	HD	WMT	JPM
AXP	1	0,69	0,61	0,47	0,48	0,49	0,65
C		1	0,57	0,45	0,49	0,52	0,72
GE			1	0,38	0,49	0,51	0,51
GM				1	0,33	0,25	0,42
HD					1	0,62	0,42
WMT						1	0,36
JPM							1

The further two clusters from each other are (correspondingly the more difference in color between two clusters is), the less the correlation coefficient between prices of stocks within these clusters are. In Tables 12 and 13 correlation coefficients for the stocks, which have fallen into the darkest blue, and the reddest clusters are given for both studied periods.

Table 12. Correlation matrix for stocks which have fallen into two most distant clusters for the period from *10-Jan-94 to 27-Oct-97*.

	AA	CAT	GM	HD	IP	WMT
JNJ	-0,03	0,16	0,14	0,19	0,07	0,16
MCD	0,04	0,20	0,04	0,17	0,05	0,07

Table 13. Correlation matrix for stocks which have fallen into two most distant clusters for the period from *10-Nov-97 to 27-Aug-01*.

	AA	CAT	EK	HON	IP	UTX
JNJ	0,07	0,17	0,04	-0,04	0,07	0,21
MRK	-0,01	0,14	0,02	0,13	0,10	0,25
PG	0,06	0,16	0,08	0,14	0,07	0,28

The given statistics shows, that the method of ultrametric spaces and the SOM method are in fair agreement for the DJIA portfolio.

6 The study of the NASDAQ100 Index by ultrametric method

In this section we investigate NASDAQ100 by ultrametric method. We obtain cluster structure of this index by building hierarchical trees.

For 100 stocks which form the NASDAQ100 (see table 14²), there are $(100 \times 99) / 2 = 4950$ different correlation coefficients ρ_{ij} . All ρ_{ij} are calculated for investigated time period from *14-Mar-01 to 31-Dec-01*. In the case of NASDAQ100 we used daily data. Maximal value of $\rho_{ij}=0,93$ characterizes two companies, developing microprocessors, namely, Novellus Systems, Inc. (NVLS) and KLA-Tencor Corporation (KLAC), (the graphs of the logarithm of stock prices of these companies are shown in Figure 14.

Table 14. The list of the stocks forming the NASDAQ100 index.

Ticker	Company	Industry sector
AAPL	Apple Computer, Inc.	Computer technique development
ABGX	Abgenix, Inc.	Biopharmaceutical industry
ADBE	Adobe Systems Inc.	Software development
ADCT	ADC Telecommunications	Telecommunication provider
ADLAC	Adelphia Communications	Communication industry
ADRX	Andrx Corporation	Biopharmaceutical industry
ALTR	Altera Corp	Software development
AMAT	Applied Materials, Inc.	Semiconductor systems development
AMCC	Applied Micro Circuits	Optic nets development
AMGN	Amgen, Inc.	Pharmaceutics industry
AMZN	Amazon.com, Inc.	IT
APOL	Apollo Group, Inc.	Higher education adults development

² finance.yahoo.com.

ATML	Atmel Corporation	IC products manufacturing
BBBY	Bed Bath & Beyond Inc.	Home improvement retailer
BEAS	BEA Systems, Inc.	Software development
BGEN	Biogen, Inc.	Biopharmaceutical industry
BMET	Biomet, Inc.	Pharmaceutics industry
BRCD	Brocade Communications	Storage area networks infrastructure production
BRCM	Broadcom Corporation	IT
CDWC	CDW Computer Centers, Inc.	High integrated silicon solutions provider
CEFT	Concord EFS, Inc.	Multi-brand computers development
CEPH	Cephalon, Inc.	Biopharmaceutical industry
CHIR	Chiron Corporation	Biopharmaceutical industry
CHKP	Check Point Software Tech	Software development
CHTR	Charter Communications	Cable systems operator
CIEN	CIENA Corporation	Optical network production
CMCSK	Comcast Corporation	Communication industry
CMVT	Comverse Technology, Inc.	Computer technique development
CNXT	Conexant Systems Inc.	Semiconductor systems development
COST	Costco Wholesale Corp.	Trading corporation
CPWR	Compuware Corporation	Software development
CSCO	Cisco Systems, Inc.	Telecommunication provider
CTAS	Cintas Corporation	Ancillary service provider
CTXS	Citrix Systems, Inc.	Software development
CYTC	CYTYC Corporation	Development of preparation system for medical applications
DELL	Dell Computer Corporation	Computer technique development
DISH	EchoStar Communications	Telecommunication provider
EBAY	eBay Inc.	IT
ERICY	LM Ericsson (ADR)	Telecommunication provider
ERTS	Electronic Arts Inc.	Software development
ESRX	Express Scripts, Inc.	Health care management
FISV	Fiserv, Inc.	Information management systems development
FLEX	Flextronics International	Telecommunication provider
GENZ	Genzyme General Division	Biotechnology development
GILD	Gilead Sciences, Inc.	Biopharmaceutical industry
GMST	Gemstar-TV Guide Intern-l	Computer technique development
HGSI	Human Genome Sciences	Therapeutic product development
ICOS	ICOS Corporation	Therapeutic product development
IDPH	IDEC Pharmaceuticals Corp	Biopharmaceutical industry
IDTI	Integrated Device Tech.	Telecommunication provider
IMCL	ImClone Systems, Inc.	Biopharmaceutical industry
IMNX	Immunex Corporation	Biopharmaceutical industry
INTC	Intel Corporation	Computer technique development
INTU	Intuit, Inc.	Software development
ITWO	I2 Technologies, Inc.	Software development
IVGN	Invitrogen Corporation	Life science market products development
JDSU	JDS Uniphase Corporation	Fiber optic components development
JNPR	Juniper Networks, Inc.	Software development
KLAC	KLA-Tencor Corporation	Semiconductor and related microelectronics development
LLTC	Linear Technology Corp.	Integrated circuits production
MCHP	Microchip Technology Inc.	Semiconductor development
MEDI	MedImmune, Inc.	Biotechnology
MERQ	Mercury Interactive Corp.	Management solutions performance
MLNM	Millennium Pharmaceutical	Biopharmaceutical industry
MOLX	Molex, Inc.	Fiber optic interconnection products manufacturer
MSFT	Microsoft Corporation	Software development
MXIM	Maxim Integrated Products	Semiconductor and related microelectronics development
NTAP	Network Appliance, Inc.	Computer technique development
NVDA	NVIDIA Corporation	Computer technique development
NVLS	Novellus Systems, Inc.	Semiconductor and related microelectronics development
NXTL	Nextel Communications	Telecommunication provider
ORCL	Oracle Corporation	Software development

PAYX	Paychex, Inc.	Financial service provider
PCAR	PACCAR Inc.	Distribution of high-quality commercial trucks
PDLI	Protein Design Labs, Inc.	Biotechnology
PMCS	PMC-Sierra, Inc.	Semiconductor and related microelectronics development
PSFT	PeopleSoft, Inc.	Software development
QCOM	QUALCOMM, Inc.	Software development
QLGC	QLogic Corporation	Semiconductor and related microelectronics development
RATL	Rational Software Corp.	Software development
RFMD	RF Micro Devices, Inc.	Integrated circuits development
SANM	Sanmina-SCI Corporation	Integrated electronic manufacturing service provider
SBUX	Starbucks Corporation	High-quality whole bean coffee roaster
SEBL	Siebel Systems, Inc.	Software development
SEPR	Sepracor Inc.	Biopharmaceutical industry
SNPS	Synopsys, Inc.	Software development
SPLS	Staples, Inc.	Office products superstore and distributor
SPOT	PanAmSat Corporation	Telecommunication provider
SSCC	Smurfit-Stone Container	Paperboard and paper-based packaging manufacturer
SUNW	Sun Microsystems, Inc.	Computer technique development
SYMC	Symantec Corporation	Network security solutions provider
TLAB	Tellabs, Inc.	Telecommunication provider
TMPW	TMP Worldwide Inc.	Advertising agency
USAI	USA Interactive	IT
VRSN	VeriSign, Inc.	Telecommunication provider
VRTS	Veritas Software Corp.	Software development
VTSS	Vitesse Semiconductor	High-performance integrated circuits development
WCOM	WorldCom Group	Telecommunication provider
XLNX	Xilinx, Incorporated	Software development
YHOO	Yahoo! Inc.	IT

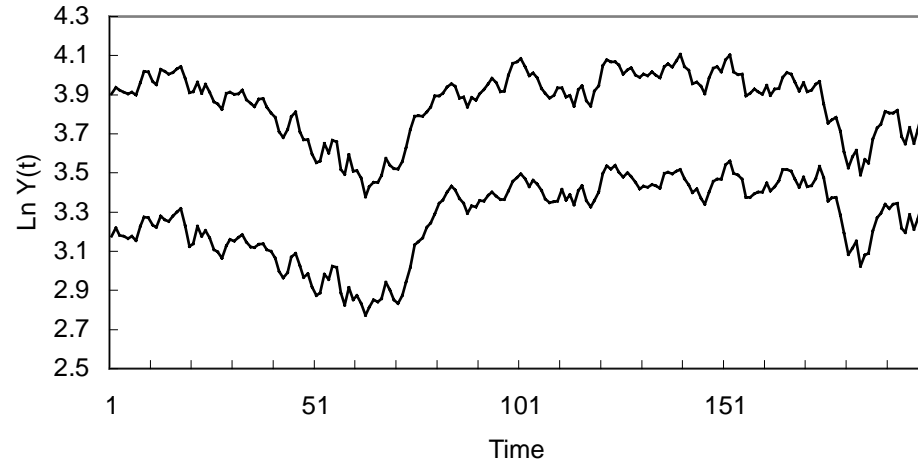


Figure 14.
LnY (t) of KLAC (the top graph) and NVLS (the bottom graph) companies
from 14-Mar-01 to 31-Dec-01.

In Figure 15 the hierarchical tree for 100 companies form NASDAQ100 index is shown. Hierarchical trees were constructed by using the Pearson distance metric and unweighted pair-group average linkage.

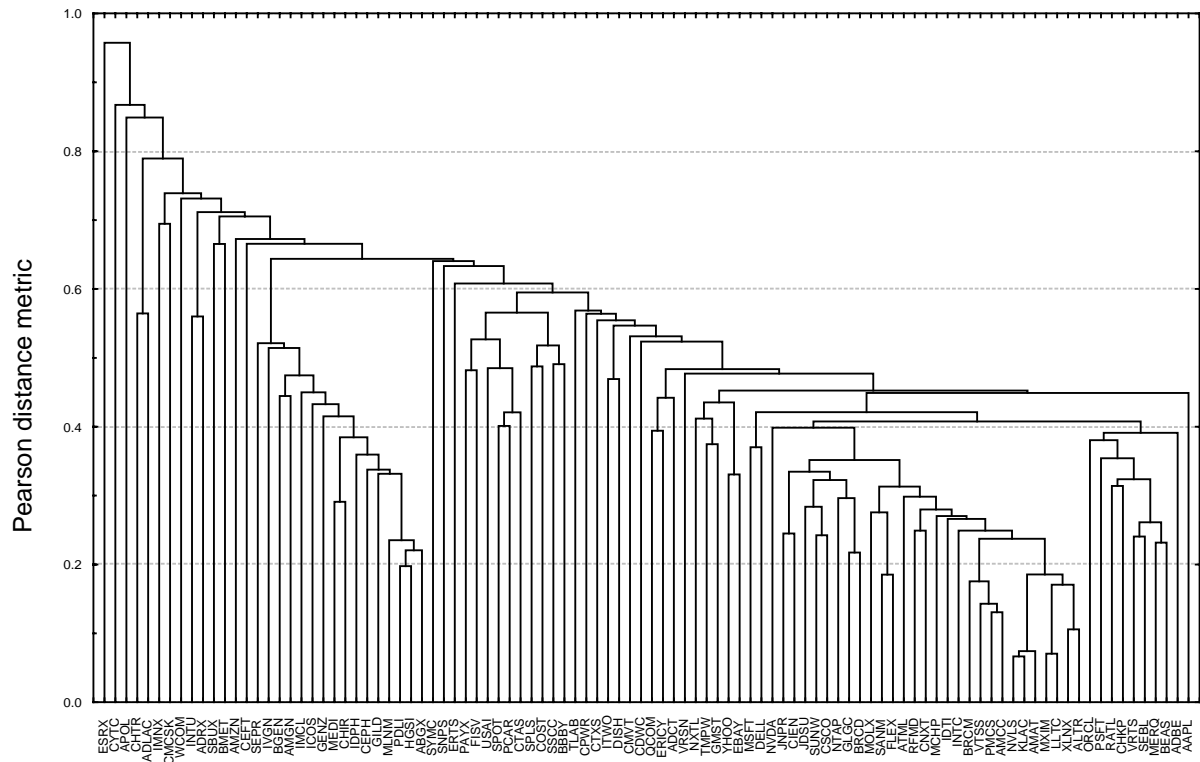


Figure 15.

The hierarchical tree for NASDAQ100 constructed by using the Pearson distance metric and unweighted pair-group average connection between clusters.

In Figure 15 one can see 4 clusters:

- SERP-IVGN-BGEN-AMGN-IMCL-ICOS-GENZ-MEDI-CHIR-IDPH-CEPH-GILD-MLNM-PDLI-HGSI-ABG X;
- PAYX-FISV-USAI-SPOT-PCAR-CTAS-SPLS-COST-SSCC-BBBY;
- JNPR-CIEN-JDSU-SUNW-CSCO-NTAP-GLGC-BRCD-MOLX-SANM-FLEX-ATML-RFMD-CNXT-MCHP-IDT I-INTC-BRCM-VTSS-PMCS-AMCC-NVLS-KLAC-AM AT-MXIM-LLTC-XLNX-ALTR
- ORCL-PSFT-RATL-CHKP-VRTS-SEBL-MERQ-BEAS-ADBE.

The most correlated cluster KLAC-NVLS-AMAT consists of the companies developing microprocessors.

7 Application of SOM method for clustering NASDAQ100

In this section we present the results obtained by neural network technology for clustering NASDAQ100 portfolio. Since the details of the approach have been described in previous sections here we restrict ourselves by expositions of results only. As quantization of NASDAQ100 is quite similar to DJIA we omit all comments and discussion, which already have been done for DJIA. In Table 15 the training parameters of SOM for NASDAQ100 are given.

Table 15. Training parameters of SOM for NASDAQ100 during the time period *14-Mar-01 to 31-Dec-01*

The size of a map	40x40 neurons
The form of cells	Hexagons
Number of epoch at the rough tuning	100000
Number of epoch at the exact tuning	100000
Learning rate at the rough tuning	0.3
Learning rate at the exact tuning	0.05
Initial radius of training	20
Final radius of training	1
Updating of the learning rate	Inversely proportional
Initial weights initialization	Random values
Time of training	4 hours and 10 minutes

In Figures 16-19 the learning error, cluster structure of SOM, U-matrix, and the error of clusterization are shown.

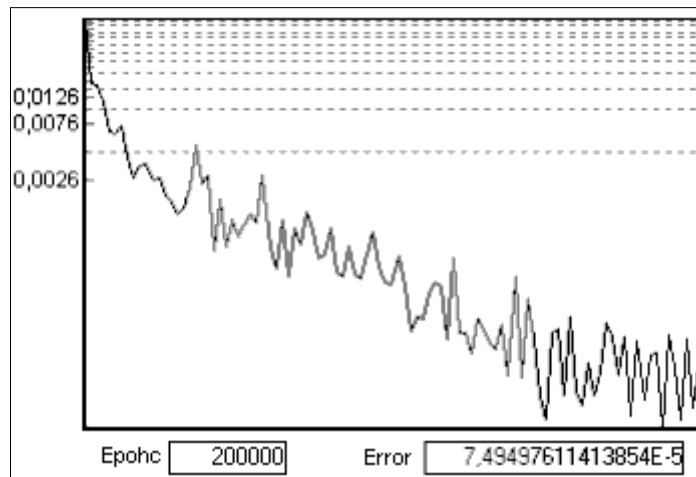


Figure 16

Learning error of SOM for NASDAQ100 during the period 10-Nov-97 to 27-Aug-01.

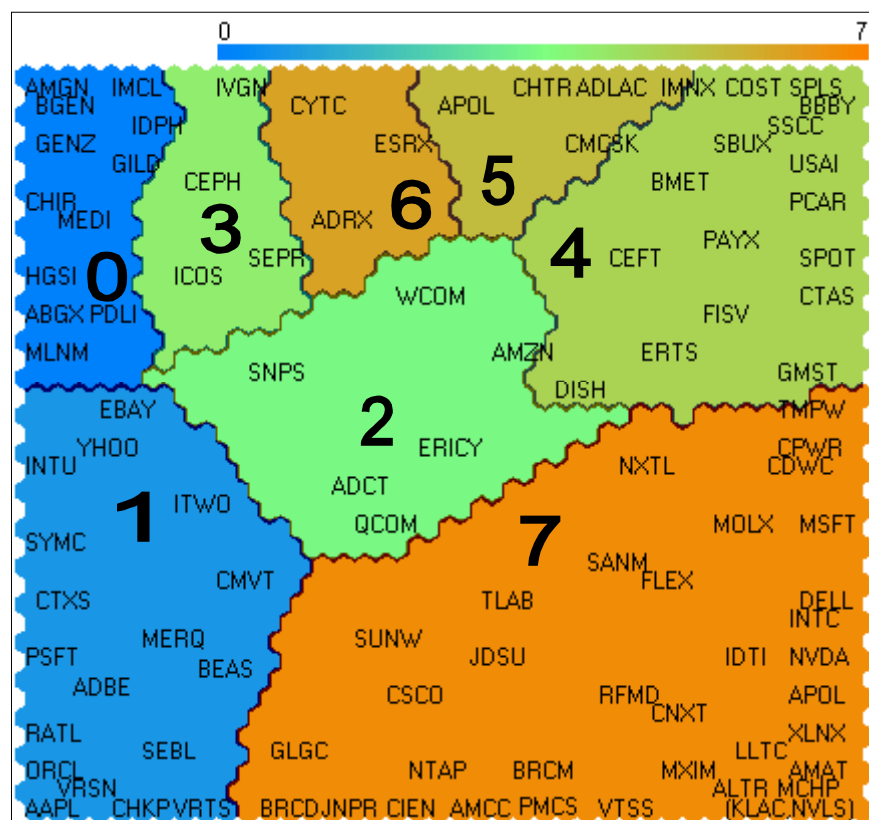


Figure 17.
Cluster structure of SOM.

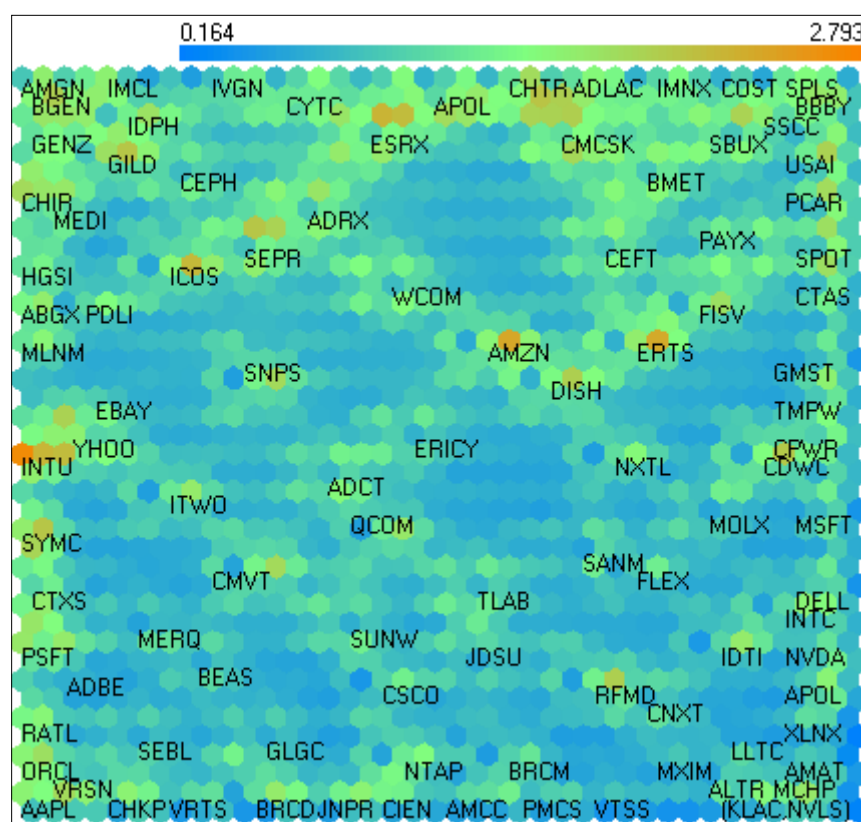


Figure 18. U-matrix.

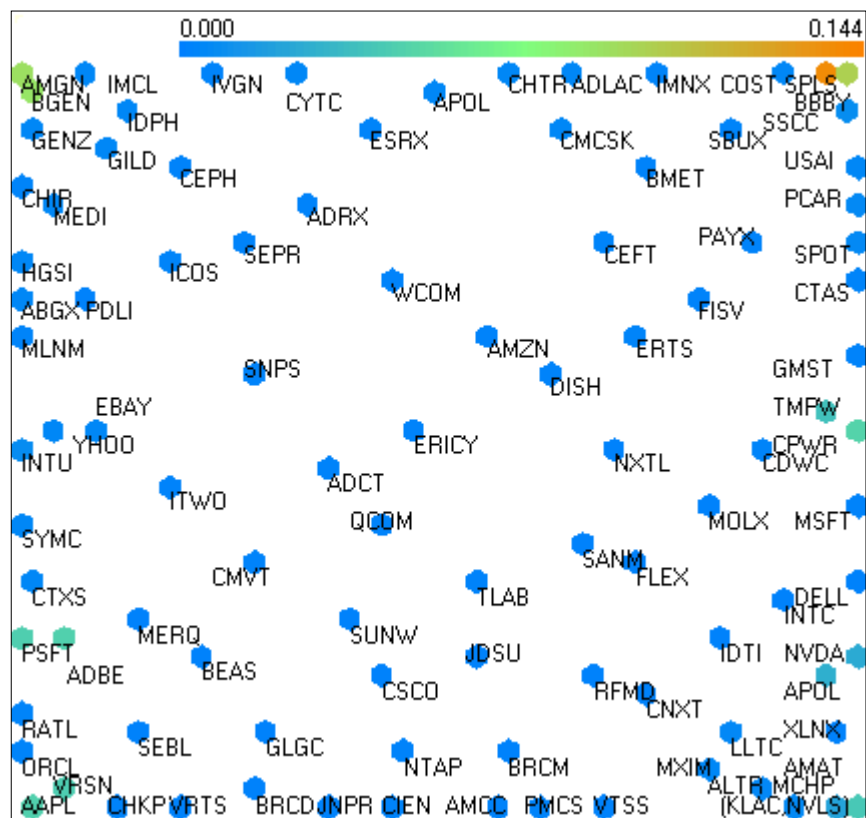


Figure 19. Error of clusterization.

One can see that due to the insufficient number of neurons (cells of the map) the U-matrix has a fuzzy structure (Fig.18). For the same reason, the more correlated stocks KLAC and NVLS have fallen into one cell. However, the statistics given below (Tables16-22), proves the successfulness of clusterization.

Table 16. The correlation matrix for stocks fallen into the cluster № 0 (see Fig.17).

	ABGX	AMGN	BGEN	CHIR	GENZ	GILD	HGSI	IDPH	IMCL	MEDI	MLNM	PDLI
ABGX	1	0.51	0.50	0.61	0.57	0.68	0.77	0.66	0.59	0.67	0.75	0.78
AMGN		1	0.56	0.56	0.49	0.54	0.59	0.57	0.43	0.61	0.53	0.54
BGEN			1	0.55	0.56	0.50	0.61	0.46	0.44	0.62	0.54	0.54
CHIR				1	0.60	0.59	0.66	0.57	0.46	0.71	0.55	0.61
GENZ					1	0.62	0.64	0.53	0.49	0.57	0.57	0.61
GILD						1	0.67	0.64	0.59	0.62	0.64	0.68
HGSI							1	0.67	0.59	0.69	0.79	0.80
IDPH								1	0.58	0.59	0.59	0.69
IMCL									1	0.51	0.58	0.63
MEDI										1	0.70	0.66
MLNM											1	0.75
PDLI												1

Table 17. Correlation matrix for stocks fallen into the cluster № 1.

	AAPL	ADBE	BEAS	CHKP	CMVT	CTXS	EBAY	INTU	ITWO	MERQ	ORCL	PSFT	RATL	SEBL	SYMC	VRSN	VRTS	YHOO
AAPL	1	0.45	0.32	0.50	0.37	0.43	0.48	0.44	0.46	0.56	0.57	0.54	0.56	0.60	0.35	0.50	0.61	0.55
ADBE		1	0.54	0.44	0.32	0.54	0.58	0.61	0.43	0.41	0.36	0.45	0.41	0.35	0.52	0.45	0.41	0.34
BEAS			1	0.52	0.64	0.23	0.53	0.63	0.51	0.64	0.42	0.62	0.52	0.56	0.53	0.42	0.65	0.58
CHKP				1	0.49	0.48	0.56	0.38	0.49	0.71	0.58	0.58	0.69	0.69	0.44	0.66	0.68	0.59
CMVT					1	0.38	0.42	0.28	0.41	0.61	0.43	0.40	0.43	0.45	0.21	0.46	0.47	0.49
CTXS						1	0.47	0.34	0.45	0.59	0.44	0.49	0.52	0.49	0.28	0.42	0.53	0.52
EBAY							1	0.39	0.50	0.63	0.49	0.46	0.60	0.58	0.38	0.51	0.53	0.67
INTU								1	0.40	0.46	0.46	0.50	0.46	0.47	0.37	0.40	0.44	0.41
ITWO									1	0.59	0.46	0.56	0.57	0.59	0.41	0.47	0.57	0.56
MERQ										1	0.64	0.70	0.73	0.76	0.53	0.55	0.73	0.66
ORCL											1	0.54	0.64	0.68	0.40	0.56	0.61	0.58
PSFT												1	0.61	0.71	0.52	0.53	0.64	0.53
RATL													1	0.67	0.39	0.58	0.61	0.61
SEBL														1	0.47	0.63	0.76	0.62
SYMC															1	0.35	0.41	0.41
VRSN																1	0.64	0.60
VRTS																	1	0.62
YHOO																		1

Table 17 includes both all stocks fallen into the most left cluster of the hierarchical tree (Fig. 15), and companies INTU, SYMC, CTXS, ITWO, CMVT, YAHOO, EBAY which are scattered on the entire hierarchical tree. It shows the interesting effect, that on the large data sets the results of linear methods (in particular, a method of ultrametric spaces) are in essential disagreement with results of nonlinear methods of SOM.

Table 18. Correlation matrix for stocks fallen into the cluster № 2.

	ADCT	AMZN	ERICY	QCOM	SNPS	WCOM
ADCT	1	0.33	0.51	0.61	0.34	0.25
AMZN		1	0.35	0.32	0.23	0.21
ERICY			1	0.61	0.42	0.39
QCOM				1	0.39	0.36
SNPS					1	0.22
WCOM						1

Table 19. Correlation matrix for stocks fallen into the cluster № 3.

	CEPH	ICOS	IVGN	SEPR
CEPH	1	0.62	0.55	0.51
ICOS		1	0.51	0.48
IVGN			1	0.44
SEPR				1

Table 20. Correlation matrix for stocks fallen into the cluster № 4.

	BBBY	BMET	CEFT	COST	CTAS	DISH	ERTS	FISV	GMST	PAYX	PCAR	SBUX	SPLS	SPOT	SSCC	USAI
BBBY	1	0.39	0.25	0.50	0.48	0.39	0.34	0.43	0.56	0.45	0.54	0.39	0.49	0.37	0.51	0.44
BMET		1	0.32	0.29	0.38	0.27	0.31	0.39	0.29	0.31	0.39	0.33	0.29	0.44	0.31	0.36
CEFT			1	0.30	0.36	0.31	0.33	0.46	0.29	0.38	0.43	0.32	0.30	0.37	0.26	0.27
COST				1	0.51	0.33	0.21	0.33	0.48	0.44	0.48	0.37	0.51	0.43	0.44	0.43
CTAS					1	0.39	0.41	0.45	0.53	0.49	0.58	0.44	0.43	0.58	0.49	0.48
DISH						1	0.38	0.41	0.44	0.36	0.43	0.34	0.37	0.36	0.42	0.42
ERTS							1	0.42	0.41	0.34	0.35	0.20	0.25	0.41	0.28	0.33
FISV								1	0.45	0.52	0.57	0.43	0.28	0.53	0.36	0.37
GMST									1	0.38	0.54	0.39	0.45	0.50	0.50	0.55
PAYX										1	0.48	0.42	0.37	0.48	0.41	0.42
PCAR											1	0.46	0.50	0.60	0.55	0.53
SBUX												1	0.39	0.43	0.32	0.37
SPLS													1	0.34	0.49	0.45
SPOT														1	0.45	0.54
SSCC															1	0.47
USAI																1

Table 21. Correlation matrix for stocks fallen into the cluster № 5.

	ADLAC	APOL	CHTR	CMCSK	IMNX
ADLAC	1	0.13	0.44	0.32	0.22
APOL		1	0.60	0.38	0.11
CHTR			1	0.28	0.14
CMCSK				1	0.31
IMNX					1

Table 22. Correlation matrix for stocks fallen into the cluster № 6.

	ADRX	CYTC	ESRX
ADRX	1	0.31	0.30
CYTC		1	0.23
ESRX			1

Table 23. Correlation matrix for the stocks fallen into the cluster № 7

	ALTR	AMAT	AMCC	APOL	BRCB	BRCM	CDWC	CIEN	CNXT	CPWR	CSCO	DELL	FLEX	IDTI	INTC	JDSU	JNPR	KLAC	LLTC	MCHP	MOLX	MSFT	MXIM	NTAP	NVDA	NVLS	NXTL	PMCS	GLGC	RFMD	SANM	SUNW	TLAB	TMPW	VTSS	XLNX
ALTR	1	0.82	0.78	0.19	0.62	0.76	0.50	0.60	0.74	0.53	0.70	0.64	0.72	0.74	0.74	0.66	0.64	0.81	0.83	0.80	0.74	0.60	0.82	0.65	0.64	0.82	0.61	0.42	0.75	0.72	0.70	0.64	0.53	0.58	0.78	0.89
AMAT	0.82	1	0.77	0.18	0.58	0.74	0.48	0.58	0.73	0.48	0.67	0.66	0.73	0.74	0.80	0.65	0.60	0.93	0.84	0.73	0.65	0.59	0.81	0.68	0.66	0.92	0.57	0.45	0.76	0.67	0.68	0.66	0.49	0.52	0.74	0.85
AMCC	0.78	0.77	1	0.15	0.65	0.82	0.45	0.72	0.73	0.46	0.75	0.61	0.68	0.73	0.74	0.76	0.75	0.76	0.77	0.66	0.67	0.61	0.77	0.72	0.64	0.73	0.59	0.46	0.77	0.73	0.68	0.65	0.53	0.58	0.87	0.78
APOL	0.19	0.18	0.15	1	0.17	0.13	0.15	0.18	0.19	0.15	0.21	0.18	0.28	0.15	0.19	0.13	0.20	0.19	0.17	0.21	0.25	0.14	0.15	0.16	0.24	0.21	0.25	0.16	0.20	0.24	0.21	0.21	0.09	0.17	0.15	0.20
BRCB	0.62	0.58	0.65	0.17	1	0.71	0.45	0.64	0.58	0.40	0.70	0.54	0.61	0.64	0.56	0.62	0.69	0.60	0.67	0.56	0.55	0.52	0.61	0.70	0.55	0.56	0.55	0.31	0.78	0.59	0.55	0.66	0.41	0.47	0.64	0.63
BRCM	0.76	0.74	0.82	0.13	0.71	1	0.47	0.69	0.74	0.43	0.75	0.61	0.70	0.73	0.73	0.74	0.73	0.73	0.76	0.70	0.68	0.61	0.76	0.72	0.63	0.73	0.65	0.41	0.77	0.72	0.71	0.67	0.49	0.58	0.82	0.74
CDWC	0.50	0.48	0.45	0.15	0.45	0.47	1	0.34	0.50	0.43	0.47	0.54	0.59	0.50	0.61	0.46	0.44	0.43	0.50	0.45	0.62	0.53	0.46	0.46	0.38	0.42	0.43	0.39	0.46	0.43	0.52	0.52	0.34	0.52	0.47	0.50
CIEN	0.60	0.58	0.72	0.18	0.64	0.69	0.34	1	0.56	0.35	0.67	0.41	0.56	0.55	0.55	0.71	0.75	0.60	0.56	0.50	0.57	0.48	0.58	0.65	0.50	0.56	0.46	0.32	0.65	0.62	0.59	0.58	0.52	0.45	0.69	0.61
CNXT	0.74	0.73	0.73	0.19	0.58	0.74	0.50	0.56	1	0.46	0.66	0.56	0.70	0.72	0.71	0.66	0.61	0.74	0.75	0.70	0.68	0.53	0.74	0.64	0.57	0.75	0.61	0.46	0.68	0.75	0.65	0.67	0.45	0.53	0.75	0.75
CPWR	0.53	0.48	0.46	0.15	0.40	0.43	0.43	0.35	0.46	1	0.50	0.43	0.48	0.49	0.53	0.42	0.39	0.47	0.49	0.50	0.51	0.47	0.49	0.42	0.44	0.49	0.52	0.35	0.47	0.37	0.44	0.44	0.37	0.50	0.44	0.44
CSCO	0.70	0.67	0.75	0.21	0.70	0.75	0.47	0.67	0.66	0.50	1	0.61	0.66	0.67	0.69	0.76	0.70	0.63	0.70	0.56	0.65	0.55	0.71	0.70	0.54	0.59	0.57	0.44	0.72	0.64	0.64	0.76	0.55	0.54	0.72	0.68
DELL	0.64	0.66	0.61	0.18	0.54	0.61	0.54	0.41	0.56	0.43	0.61	1	0.59	0.62	0.71	0.58	0.53	0.62	0.70	0.58	0.64	0.63	0.66	0.55	0.61	0.61	0.52	0.43	0.62	0.52	0.53	0.56	0.39	0.57	0.57	0.66
FLEX	0.72	0.73	0.68	0.28	0.61	0.70	0.59	0.56	0.70	0.48	0.66	0.59	1	0.69	0.74	0.67	0.62	0.69	0.70	0.69	0.72	0.59	0.68	0.64	0.53	0.73	0.68	0.50	0.71	0.68	0.81	0.67	0.49	0.62	0.71	0.71
IDTI	0.74	0.74	0.73	0.15	0.64	0.73	0.50	0.55	0.72	0.49	0.67	0.62	0.69	1	0.70	0.63	0.62	0.73	0.80	0.72	0.62	0.53	0.76	0.66	0.64	0.72	0.65	0.46	0.74	0.67	0.65	0.67	0.49	0.56	0.74	0.73
INTC	0.74	0.80	0.74	0.19	0.56	0.73	0.61	0.55	0.71	0.53	0.69	0.71	0.74	0.70	1	0.68	0.58	0.74	0.79	0.69	0.74	0.69	0.75	0.63	0.64	0.74	0.59	0.41	0.69	0.66	0.69	0.70	0.45	0.59	0.72	0.77
JDSU	0.66	0.65	0.76	0.13	0.62	0.74	0.46	0.71	0.66	0.42	0.76	0.58	0.67	0.63	0.68	1	0.67	0.61	0.68	0.58	0.65	0.52	0.71	0.67	0.53	0.59	0.55	0.43	0.68	0.64	0.68	0.68	0.60	0.54	0.73	0.66
JNPR	0.64	0.60	0.75	0.20	0.69	0.73	0.44	0.75	0.61	0.39	0.70	0.53	0.62	0.62	0.58	0.67	1	0.61	0.64	0.53	0.61	0.52	0.66	0.65	0.55	0.58	0.57	0.38	0.74	0.64	0.62	0.62	0.48	0.54	0.70	0.60
KLAC	0.81	0.93	0.76	0.19	0.60	0.73	0.43	0.60	0.74	0.47	0.63	0.62	0.69	0.73	0.74	0.61	0.61	1	0.82	0.76	0.63	0.55	0.78	0.66	0.63	0.93	0.57	0.42	0.75	0.70	0.65	0.62	0.49	0.50	0.76	0.83
LLTC	0.83	0.84	0.77	0.17	0.67	0.76	0.50	0.56	0.75	0.49	0.70	0.70	0.70	0.80	0.79	0.68	0.64	0.82	1	0.74	0.70	0.61	0.93	0.66	0.72	0.80	0.61	0.45	0.81	0.73	0.70	0.66	0.48	0.59	0.78	0.84
MCHP	0.80	0.73	0.66	0.21	0.56	0.70	0.45	0.50	0.70	0.50	0.56	0.58	0.69	0.72	0.69	0.58	0.53	0.76	0.74	1	0.67	0.50	0.71	0.55	0.58	0.80	0.61	0.42	0.66	0.67	0.61	0.55	0.49	0.48	0.72	0.76
MOLX	0.74	0.65	0.67	0.25	0.55	0.68	0.62	0.57	0.68	0.51	0.65	0.64	0.72	0.62	0.74	0.65	0.61	0.63	0.70	0.67	1	0.70	0.68	0.58	0.58	0.65	0.64	0.51	0.68	0.67	0.73	0.59	0.51	0.66	0.68	0.73
MSFT	0.60	0.59	0.61	0.14	0.52	0.61	0.53	0.48	0.53	0.47	0.55	0.63	0.59	0.53	0.69	0.52	0.52	0.55	0.61	0.50	0.70	1	0.62	0.57	0.51	0.57	0.56	0.41	0.57	0.53	0.59	0.51	0.34	0.61	0.58	0.61
MXIM	0.82	0.81	0.77	0.15	0.61	0.76	0.46	0.58	0.74	0.49	0.71	0.66	0.68	0.76	0.75	0.71	0.66	0.78	0.93	0.71	0.68	0.62	1	0.67	0.69	0.77	0.58	0.46	0.80	0.70	0.69	0.65	0.50	0.59	0.79	0.82
NTAP	0.65	0.68	0.72	0.16	0.70	0.72	0.46	0.65	0.64	0.42	0.70	0.55	0.64	0.66	0.63	0.67	0.65	0.66	0.66	0.55	0.58	0.57	0.67	1	0.57	0.63	0.50	0.36	0.71	0.60	0.58	0.69	0.50	0.49	0.71	0.67
NVDA	0.64	0.66	0.64	0.24	0.55	0.63	0.38	0.50	0.57	0.44	0.54	0.61	0.53	0.64	0.64	0.53	0.55	0.63	0.72	0.58	0.58	0.51	0.69	0.57	1	0.63	0.48	0.36	0.69	0.58	0.52	0.52	0.37	0.46	0.60	0.68
NVLS	0.82	0.92	0.73	0.21	0.56	0.73	0.42	0.56	0.75	0.49	0.59	0.61	0.73	0.72	0.74	0.59	0.58	0.93	0.80	0.80	0.65	0.57	0.77	0.63	0.63	1	0.61	0.47	0.72	0.71	0.67	0.58	0.47	0.54	0.75	0.83
NXTL	0.61	0.57	0.59	0.25	0.55	0.65	0.43	0.46	0.61	0.52	0.57	0.52	0.68	0.65	0.59	0.55	0.57	0.57	0.61	0.61	0.64	0.56	0.58	0.50	0.48	0.61	1	0.47	0.59	0.59	0.65	0.53	0.47	0.60	0.61	0.56
PMCS	0.42	0.45	0.46	0.16	0.31	0.41	0.39	0.32	0.46	0.35	0.44	0.43	0.50	0.46	0.41	0.43	0.38	0.42	0.45	0.42	0.51	0.41	0.46	0.36	0.36	0.47	0.47	1	0.43	0.42	0.48	0.33	0.25	0.48	0.42	0.48
GLGC	0.75	0.76	0.77	0.20	0.78	0.77	0.46	0.65	0.68	0.47	0.72	0.62	0.71	0.74	0.69	0.68	0.74	0.75	0.81	0.66	0.68	0.57	0.80	0.71	0.69	0.72	0.59	0.43	1	0.70	0.66	0.66	0.42	0.53	0.72	0.75
RFMD	0.72	0.67	0.73	0.24	0.59	0.72	0.43	0.62	0.75	0.37	0.64	0.52	0.68	0.67	0.66	0.64	0.64	0.70	0.73	0.67	0.67	0.53	0.70	0.60	0.58	0.71	0.59	0.42	0.70	1	0.66	0.59	0.44	0.48	0.75	0.72
SANM	0.70	0.68	0.68	0.21	0.55	0.71	0.52	0.59	0.65	0.44	0.64	0.53	0.81	0.65	0.69	0.68	0.62	0.65	0.70	0.61	0.73	0.59	0.69	0.58	0.52	0.67	0.65	0.48	0.66	0.66	1	0.64	0.58	0.61	0.72	0.68
SUNW	0.64	0.66	0.65	0.21	0.66	0.67	0.52	0.58	0.67	0.44	0.76	0.56	0.67	0.67	0.70	0.68	0.62	0.62	0.66	0.55	0.59	0.51	0.65	0.69	0.52	0.58	0.53	0.33	0.66	0.59	0.64	1	0.53	0.53	0.68	0.65
TLAB	0.53	0.49	0.53	0.09	0.41	0.49	0.34	0.52	0.45	0.37	0.55	0.39	0.49	0.49	0.45	0.60	0.48	0.49	0.48	0.49	0.51	0.34	0.50	0.50	0.37	0.47	0.47	0.25	0.42	0.44	0.58	0.53	1	0.42	0.54	0.48
TMPW	0.58	0.52	0.58	0.17	0.47	0.58	0.52	0.45	0.53	0.50	0.54	0.57	0.62	0.56	0.59	0.54	0.54	0.50	0.59	0.48	0.66	0.61	0.59	0.49	0.46	0.54	0.60	0.48	0.53	0.48	0.61	0.53	0.42	1	0.59	0.56
VTSS	0.78	0.74	0.87	0.15	0.64	0.82	0.47	0.69	0.75	0.44	0.72	0.57	0.71	0.74	0.72	0.73	0.70	0.76	0.78	0.72	0.68	0.58	0.79	0.71	0.60	0.75	0.61	0.42	0.72	0.75	0.72	0.68	0.54	0.59	1	0.78
XLNX	0.89	0.85	0.78	0.20	0.63	0.74	0.50	0.61	0.75	0.44	0.68	0.66	0.71	0.73	0.77	0.66	0.60	0.83	0.84	0.76	0.73	0.61	0.82	0.67	0.68	0.83	0.56	0.48	0.75	0.72	0.68	0.65	0.48	0.56	0.78	1

Table 24. Correlation matrix for the stocks which fallen into the 0-th and 7-th clusters.

	ALTR	AMAT	AMCC	APOL	BRCB	BRCM	CDWC	CIEN	CNXT	CPWR	CSCO	DELL	FLEX	IDTI	INTC	JDSU	JNPR	KLAC	LLTC	MCHP	MOLX	MSFT	MXIM	NTAP	NVDA	NVLS	NXTL	PMCS	GLGC	RFMD	SANM	SUNW	TLAB	TMPW	VTSS	XLNX
ABGX	0.48	0.52	0.46	0.18	0.35	0.47	0.39	0.38	0.53	0.34	0.43	0.46	0.53	0.47	0.49	0.47	0.43	0.49	0.48	0.50	0.55	0.40	0.48	0.39	0.36	0.53	0.48	0.43	0.48	0.48	0.52	0.39	0.25	0.43	0.45	0.54
AMGN	0.29	0.37	0.33	0.14	0.13	0.22	0.28	0.23	0.37	0.23	0.30	0.30	0.32	0.26	0.35	0.33	0.26	0.37	0.35	0.27	0.41	0.28	0.37	0.27	0.21	0.34	0.29	0.30	0.27	0.29	0.32	0.24	0.21	0.34	0.28	0.37
BGEN	0.29	0.36	0.31	0.34	0.15	0.21	0.26	0.24	0.30	0.22	0.19	0.23	0.30	0.25	0.30	0.27	0.19	0.34	0.33	0.29	0.39	0.32	0.34	0.21	0.23	0.30	0.24	0.27	0.26	0.22	0.29	0.15	0.13	0.23	0.23	0.40
CHIR	0.35	0.43	0.39	0.17	0.19	0.32	0.28	0.23	0.37	0.30	0.35	0.40	0.40	0.32	0.39	0.34	0.31	0.42	0.42	0.31	0.47	0.42	0.43	0.30	0.28	0.41	0.36	0.34	0.36	0.32	0.44	0.29	0.18	0.42	0.34	0.43
GENZ	0.37	0.38	0.39	0.15	0.23	0.32	0.30	0.33	0.33	0.35	0.26	0.31	0.39	0.32	0.33	0.32	0.30	0.39	0.33	0.38	0.45	0.34	0.38	0.33	0.31	0.41	0.31	0.32	0.35	0.33	0.34	0.24	0.16	0.41	0.36	0.38
GILD	0.31	0.39	0.34	0.16	0.22	0.33	0.31	0.25	0.37	0.26	0.31	0.33	0.46	0.32	0.31	0.37	0.33	0.37	0.37	0.37	0.40	0.26	0.38	0.26	0.31	0.39	0.42	0.29	0.35	0.34	0.42	0.23	0.18	0.40	0.32	0.35
HGSI	0.48	0.57	0.54	0.10	0.40	0.49	0.44	0.40	0.55	0.39	0.48	0.48	0.55	0.53	0.52	0.48	0.43	0.53	0.53	0.49	0.55	0.44	0.54	0.42	0.41	0.53	0.50	0.49	0.50	0.50	0.51	0.42	0.29	0.45	0.47	0.57
IDPH	0.31	0.33	0.35	0.11	0.18	0.29	0.25	0.23	0.32	0.22	0.31	0.31	0.37	0.30	0.27	0.30	0.31	0.32	0.31	0.32	0.36	0.25	0.34	0.25	0.22	0.34	0.30	0.30	0.36	0.29	0.39	0.21	0.16	0.38	0.29	0.36
IMCL	0.26	0.30	0.30	0.18	0.22	0.27	0.28	0.21	0.30	0.27	0.30	0.32	0.39	0.29	0.27	0.34	0.30	0.30	0.30	0.27	0.37	0.26	0.31	0.25	0.24	0.30	0.37	0.25	0.32	0.31	0.33	0.23	0.21	0.39	0.26	0.28
MEDI	0.47	0.52	0.50	0.23	0.31	0.42	0.33	0.38	0.51	0.38	0.44	0.42	0.49	0.38	0.48	0.46	0.42	0.48	0.48	0.44	0.61	0.48	0.49	0.36	0.36	0.51	0.45	0.44	0.47	0.40	0.46	0.36	0.27	0.48	0.46	0.53
MLNM	0.54	0.54	0.53	0.21	0.43	0.52	0.46	0.46	0.55	0.44	0.54	0.51	0.58	0.50	0.51	0.53	0.48	0.53	0.51	0.52	0.60	0.50	0.54	0.45	0.35	0.54	0.58	0.49	0.53	0.50	0.56	0.45	0.35	0.52	0.48	0.56
PDLI	0.42	0.45	0.46	0.16	0.31	0.41	0.39	0.32	0.46	0.35	0.44	0.43	0.50	0.46	0.41	0.43	0.38	0.42	0.45	0.42	0.51	0.41	0.46	0.36	0.36	0.47	0.47	0.39	0.43	0.42	0.48	0.33	0.25	0.48	0.42	0.48

In Table 24 correlation coefficients between the companies, which have fallen into the darkest blue and reddest clusters (the distance between these clusters is maximum) are given. The mean value and the standard deviation of the correlation matrix for the companies forming NASDAQ100 are equal to 0.47 and 0.18 correspondingly. Mean value of correlation coefficients from Table 24, is equal to 0.37. As one would expect, average value of correlation coefficients between companies, which have fallen into clusters №0 and №7 is less then the average of all coefficients of correlations.

8 Conclusion

The paper shows advantages of self-organizing maps in comparison with traditional models of statistical data analysis. In particular we compare the clusterization of DJIA and NASDAQ100 portfolios by hierarchical trees and SOM methods. It was shown, that:

1. In the case of DJIA the results of both methods appeared quite similar. It means that ultrametric methods practically do not lead to an error in clusterization on a small data sample.
2. The clusterization of NASDAQ100 shows that the results of SOM are essentially subtle than methods of ultrametrics. Such results mean, in particular, that conventional statistical methods are imperfect in application to the large data samples.

Thus one can conclude that the SOM method is more relevant to the problems where processing of the large data samples is required. In particular, this method can be used for the forming and dynamical management a well diversified portfolio of stocks.

9 References

1. Kohonen, T. (1982) Self-organized formation of topologically correct feature maps. *Biological Cybernetics*, **43**:59-69.
2. Kohonen, T. (1990) The Self-Organizing Map. *Proceeding of the IEEE*, **78**:1464-1480.
3. Kohonen, T. (1995) *The Self-Organizing Maps*. Springer, Berlin.
4. Kohonen, T., Oja, E., Simula, O., Visa, A. and Kangas, J. (1996). Engineering applications of the self-organizing map. *Proceedings of IEEE*, **84**:1358-1389.
5. Back, B., Sere, K., and Vanharanta, H. (1996) Data mining accounting numbers using self-organizing maps. (Alander, J., Honkela, T., and Jakobsson, M., Eds.), *Proceedings of STeP'96, Finnish artificial Intelligence Conference*, pages 35-47. Finnish Artificial Intelligence Society, Vaasa, Finland.
6. Demartines, P. (1994) *Analyse de données par réseaux de neurons auto-organisés (Data analysis through self-organized neural networks)*. PhD thesis, Institut National Polytechnique de Grenoble, Grenoble, France.
7. Carlson, E. (1991) Self-organizing feature maps for appraisal of land value of shore parcels. (Kohonen, T., Mäkisara, K., Simula, O., and Kangas, J., Eds.), *Artificial Neural Networks. Proceedings of ICANN'91, International Conference on Artificial Neural Networks*, volume II, pages 1309-1312, North-Holland, Amsterdam.
8. Cheng, G., Liu, X., and Wu, J.X. (1994) Interactive knowledge discovery through self-organizing feature maps. In *Proceedings of WCNN'94, World Congress on Neural Networks*, volume IV, pages 430-434. Lawrence Erlbaum, Hillsdale, NJ.
9. Garavaglia, S. (1993) A self-organizing map applied to macro and microanalysis of data with dummy variables. In *Proceedings of WCNN'93, World Congress on Neural Networks*, pages 362-368. Lawrence Erlbaum and INNS Press, Hillsdale, NJ.
10. Martín-del-Brío, B. and Serrano-Cinca, C. (1993) Self-organizing neural networks for the analysis and representation of data: some financial cases. *Neural Computing & Applications*, **1**:193-206.
11. Marttinen, K. (1993) SOM in statistical analysis: supermarket customer profiling. (Bulsari, A. and Saxén, B., Eds.), *Proceedings of the Symposium on Neural Network Research in Finland*, pages 75-80. Finnish Artificial Intelligence Society, Turku, Finland.
12. Serrano-Cinca, C. (1996) Self-organizing neural networks for financial diagnosis. *Decision Support Systems*.
13. Ultsch, A. (1993) Self-organizing neural networks for visualization and classification. (Opitz, O., Lausen, B., and Klar, R., Eds.) *Information and Classification*, pages 307-313. Springer-Verlag, Berlin.
14. Ultsch, A. and Siemon, H. P. (1990) Kohonen's self-organizing feature maps for exploratory data analysis. In *Proceedings of ICNN'90, International Neural Network Conference*, pages 305-308, Kluwer, Dordrecht.
15. Varfis, A. and Versino, C. (1992) Clustering of socio-economic data with Kohonen maps. *Neural Network World*, **2**:813-834.
16. Zhang, X. and Li, Y. (1993) Self-organizing map as a new method for clustering and data analysis. In *Proceedings of IJCNN'93 (Nagoya), International Joint Conference on Artificial Neural Networks*, pages 2448-2451, IEEE Service Center, Piscataway, NJ.
17. Deboeck G., Kohonen T. (1998) *Visual Exploration in Finance with Self-Organizing Maps*, Springer – Verlag.
18. Ezhov A.A., Shumsky S.A. “Neurocomputing and its application in economics and business. Moscow: MEPHI, 1998 (in Russian).
19. Kaski, S., (1997) Data exploration using self-organizing maps. *Acta Polytechnica Scandinavica, Mathematics, Computing and Management in Engineering Series No. 82, Espoo*, 57 pp. Published by the Finnish Academy of Technology.
20. S.A. Terekhov, (1997) “Neural-engineering models of complex systems”, SPb, SETU.

21. J. Kangas, (1994) "On the Analysis of Pattern Sequences by Self-Organizing Maps". PhD thesis, Helsinki University of Technology, Espoo, Finland.
22. Oja E., Ogawa H., Wangviwattana J., (1991) "Learning in nonlinear constrained Hebbian network", (Kohonen T., et al. Eds.), "Artificial neural networks", North-Holland, Amsterdam, p. 385.
23. R. N. Mantegna, H. E. Stanley, (2001) "An Introduction to Econophysics – Correlation and Complexity in Finance", Cambridge University Press.
24. J. P. Benzécri, (1984) "L'analyse des données 1, La Taxionomie" (Dunod, Paris).
25. R. Rammal, G. Toulouse, and M.A. Virasoro, (1986) "Ultrametricity for Physicists", *Rev. Mod. Phys.* 58, 765-788.
26. StatSoft, Inc.2001 WEB: http://www.statsoft.ru/home/portal/textbook_ind/default.htm.
27. R. N. Mantegna, (1997) "Degree of Correlation Inside a Financial Market", in Applied Nonlinear Dynamics and Stochastic Systems near the Millennium, Edited by J.B.Kadtke and A. Bulsara (AIP Press, New York), pp.197-202.
28. T. Graepel, M. Burger, K. Obermayer, (1998) "Self-Organizing Maps: Generalizations and New Optimization Techniques", *Neurocomputing*, **20**:173-190.